ELSEVIER

Surface Science 398 (1998) 37–48

surface science

Decay of Cu adatom islands on Cu(111)

G. Schulze Icking-Konert, M. Giesen, H. Ibach *

Institut für Grenzflächenforschung und Vakuumphysik, Forschungszentrum Jülich, D-52425 Jülich, Germany

Received 3 July 1997; accepted for publication 16 October 1997

Abstract

We have investigated the decay of Cu adatom islands on Cu(111) as a function of temperature using scanning tunneling microscopy. By comparing the experimental results with the theory of Ostwald ripening and with numerical simulations we find that the decay is limited by the diffusion of adatoms on the terrace. From the decay rate at constant island size as a function of temperature, the sum of the energy for the formation of an adatom on the terrace and the activation energy for diffusion on the terrace is found to be 0.78 ± 0.04 eV. The local environment has a significant influence on the shape of the island area versus time curves. An optimum match between simulations and experiment for the shape of the decay curves is achieved for a line tension of the islands of 0.45 eV per atom length. The Schwoebel–Ehrlich barrier for the hopping of atoms over a step is determined to be about 0.12 eV by matching the relative decay times of islands on small terraces to the simulations. © 1998 Elsevier Science B.V.

Keywords: Computer simulations; Nonequilibrium thermodynamics; Scanning tunneling microscopy; Surface diffusion; Surface morphology

1. Introduction

The formation and stability of nanostructures on surfaces has attracted considerable interest recently [1–6]. While substantial effort was devoted to the growth kinetics [5–7], relatively little is known about the (long-term) stability of nanostructures. An assessment of the stability requires an understanding of the nature of the processes responsible for the decay of nano-structures and furthermore a precise knowledge of the activation energies involved in the relevant processes. Recently, Morgenstern et al. have shown that quantitative studies of the decay of two-dimensional islands on an Ag(111) surface can provide information on the energetics governing the decay [1,8]. In particular, these authors have determined the line tension of islands from a measurement of the shape of the island decay curves versus time. The present study is an extension of their pioneering work to the Cu(111) surface. Specifically, we show that an extraction of the line tension from the island decay curves with the help of simple analytical solutions of the theory of Ostwald ripening is not possible for general geometries because the shape of the decay curves depends more significantly on the environment of an island than on the line tension. We will show that the line tension, nevertheless, can be extracted from the data by a numerical simulation of the decay process of an entire ensemble of islands. For islands in the vicinity of a descending step, for islands on top of another island, as well

* Corresponding author. Tel: (+49) 2461 614561; fax: (+49) 2461 613907; e-mail: h.ibach@fz-juelich.de

PII S0039-6028(97)00755-3

as for mound-like structures, the decay rate depends on the magnitude of the activation barrier for hopping over a step edge. Quite frequently, this activation barrier is larger than the barrier for the diffusion of adatoms over the terrace (Schwoebel–Ehrlich barrier [9,10]). The presence of a Schwoebel–Ehrlich barrier has a significant effect on the growth morphology [11,12] since layer-by-layer growth requires an interlayer mass transport. We have determined the activation energy for the hopping over the Schwoebel–Ehrlich barrier to about 0.12 eV from a comparison of the relative lifetimes of islands on small terraces in simulations and experiments. From the temperature dependence of the decay rate of islands at constant island size the sum of the energy for the formation of an adatom on a terrace from a step and the activation barrier for the diffusion on a terrace is determined to 0.78 eV.

The paper is organized as follows. In Section 2, the experimental set-up is described. The experimental results are presented in Section 3. A brief summary of the theory of Ostwald ripening as well as the method and the results of numerical simulations are described in Section 4. The paper concludes with a comparison of the various energies obtained from the analysis of the experimental data to theoretical calculations.

2. Experimental

Our temperature variable scanning tunneling microscope (STM) of the Besocke type [13] is part of a standard UHV chamber with a base pressure of typically 5×10^{-11} mbar. The sample temperature can be varied radiatively and by electron beam heating. The UHV chamber is equipped with an electron beam evaporator (Omicron EFM3) for the copper deposition on the sample surface. The calibration of the evaporator has been performed by MEED oscillations in a geometrically identical chamber. Once the evaporator is calibrated, the deposition rate can be determined from the measured ion flux. Special care was taken to degas the evaporator and the Cu source so that during deposition the pressure in the chamber never exceeded 1×10^{-10} mbar.

The single crystal used in this experiment was cut by spark erosion and polished mechanically to an accuracy of 0.1°. Its sulfur content was leached by heating in a 1:25 hydrogen and argon atmosphere at 800°C for several hours prior to mounting in the UHV chamber. The final sample preparation in the UHV chamber was performed by repeated cycles of sputtering with Ne^+ at 1 kV for 10 min (5 μA ion current) and successive annealing at 700°C for another 10 min. The temperature was then lowered to below 100°C before starting the next cycle. To minimize thermally induced strain, the single crystal was cooled down over a period of 10 min. After a few cycles, no contamination was detectable in the Auger spectrum. Since island decay is rather sensitive to contamination, a surface coverage below the detection limit of Auger spectroscopy may still have a non-negligible influence on the measurements. We therefore continued the cleaning procedure many cycles beyond the point at which we found the sample clean by Auger standards. The final state of the surface after the preparation procedure was controlled by means of the STM images.

After the final cycle, the sample was cooled down slowly to the temperature at which the measurement was performed. In order to minimize thermal drift in the STM images, the sample was allowed to equilibrate thermally for approximately 30 min prior to deposition of Cu. Typically, 0.5–1 monolayers (ML) Cu were deposited at a rate of 2 ML/min. The sample was then placed onto the STM and the STM tip was brought into tunneling range within 10 min after deposition. Typical scan parameters were 1.2 nA, −1.0 V and a scan speed of 60 s per 512×512 pixel image. Since no measurable influence on equilibrium step fluctuations was found on Cu(111) surfaces using similar tunneling parameters [14], the tip–surface interactions are negligible for this system. A complete series of images took between 2 and 11 h to record, depending on the sample temperature.

3. Experimental results

The sizes of Cu adatom islands have been recorded as a function of time and temperature.

A typical series of STM images is shown in Fig. 1. An electronic high-pass filter was applied to the recorded signal while scanning to correct for the tilt of the sample. Thus, the islands appear as if illuminated from the left hand side. In order to analyze the STM images we used a special purpose computer code which allows for the simultaneous evaluation of the size of all islands in an image. The program fits a spline to the gray values of each scan line and searches for the largest slopes in this spline. Non-physical large jumps in the island edge due to noise are filtered out. In order to test the scaling of the areas found by the program we have recorded images of islands with different scan widths and evaluated the island area using the program. The areas of the islands in pixels as determined by the program were then compared with the areas expected from the nominal scaling of the STM. No deviation was found.

We have measured the time dependence of the island sizes between 300 and 355 K. The STM image of a particular set of islands in its initial stage at 308 K is shown in Fig. 2. In this particular example, the islands are deposited on a section of the surface with relatively narrow terraces, separated by (100) oriented steps (A-type steps). Such an island distribution is particular suitable for a numerical analysis, as discussed later. The islands in Fig. 2 were produced by depositing several monolayers of Cu. As a consequence, one has small vacancy islands on the terraces in addition to the adatom islands. Despite their smallness, the vacancy islands persist for quite some time which is evidence for the existence of a Schwoebel–Ehrlich barrier for the hopping of adatoms over a descending step. The asymmetry of the island decay with regard to the steps displayed in Fig. 1 is likewise evidence for the existence of a

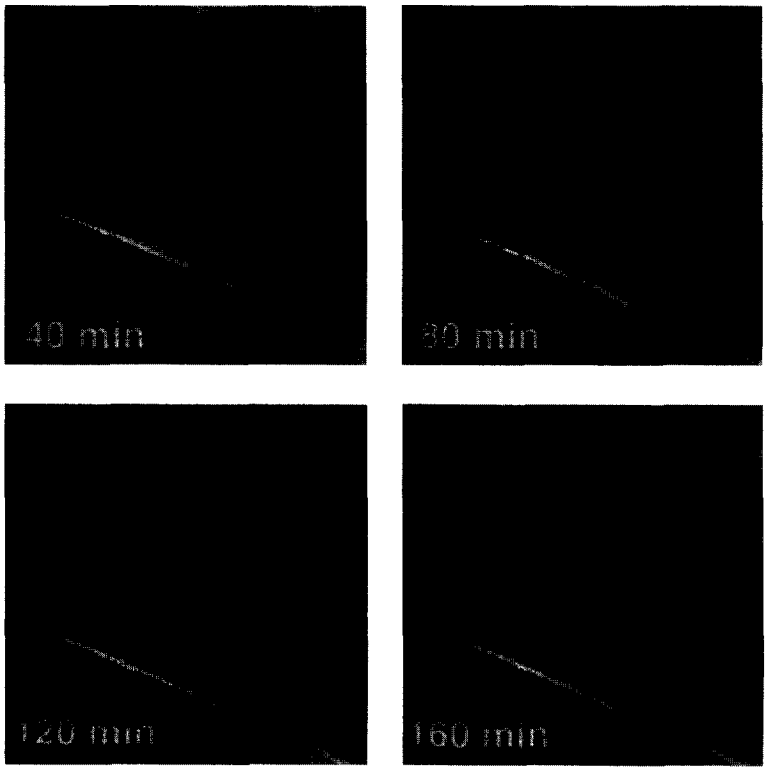

Fig. 1. Series of STM-images of Cu/Cu(111) taken at $T=319$ K and a scan width of 4000×4000 Å. Tunneling parameters are $I_t=1.4$ nA; $U_t=-1.2$ V. The times indicated in the images refer to the deposition time. Some of the islands decay as time progresses. The depletion zone near upward steps and the missing of such a zone near downward steps is again evidence for the existence of a Schwoebel–Ehrlich barrier.

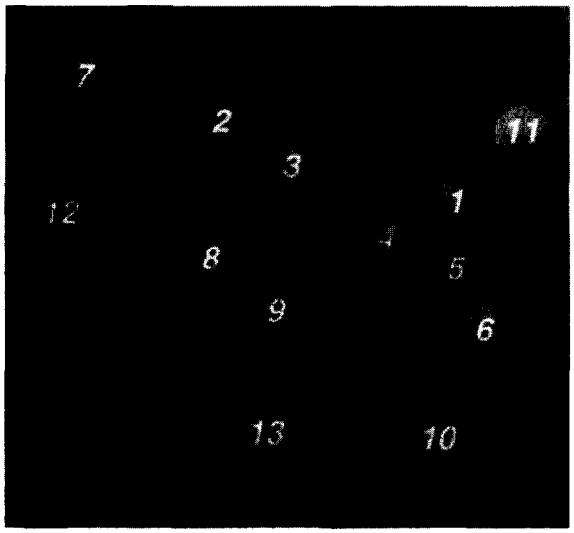

Fig. 2. A distribution of islands on narrow terraces. The steps are (100) oriented (A-type steps). The islands are produced by deposition of several monolayers. At 308 K, the small vacancy islands on the terraces are filled only very gradually by the adatoms which is evidence for a the presence of a Schwoebel–Ehrlich barrier.

Schwoebel–Ehrlich barrier. At the ascending step, the island free zone widens as time progresses, while no such denuded zone develops near the descending step. Hence islands close to a descending step decay less rapidly than islands at an ascending step.

Fig. 3 shows the evolution of island sizes in time at 308 K for several of the islands in Fig. 2. The late stages of the decay are well described by a power law:

$$A(t)=A(0)(1-t/t_0)^{\kappa}. \quad (1)$$

From a least-square fit to many islands (mostly well apart from steps) the average scaling exponent κ was found to be 0.54 ± 0.04. Within the error bar, the exponent was also found to be independent of temperature. Contrary to what was assumed in Ref. [1], this mean exponent of 0.54 is not amenable to a quantitative interpretation since the exponents for individual islands depend significantly on the environment of each island. Table 1 shows the exponents κ for a few islands in Fig. 2 as an example. The difference between an island which is surrounded by other islands – for example,

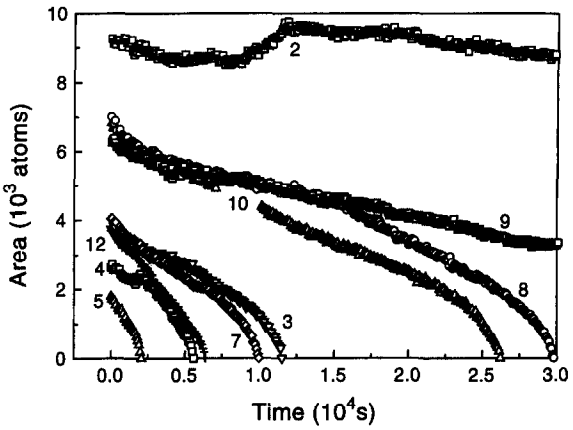

Fig. 3. Island sizes in 370 STM images versus time for the group of islands shown in Fig. 2 at a temperature of 308 K. The islands are numbered as in Fig. 2. The interaction between islands is quite apparent as an increase in island size when a neighboring island is close to the point of extinction (see island 4, when island 5 disappears and island 2, when island 3 disappears).

Table 1
Experimental decay exponents κ [Eq. (1)] for various islands in Fig. 2. The exponents were determined using the data in the later stages of the island's life

Island	κ
3	0.57
4	0.67
5	0.58
8	0.57
12	0.73

island 5 and an island which is close to an ascending step, i.e. island 12 – is particularly large. The strong dependence of κ on the environment is characteristic for the diffusion limited decay. We address this issue later in detail in connection with the simulations. The interaction between neighboring islands and the effect of the interaction on the decay is also visible in Fig. 3. Island 2, for example, decays initially, then grows as the neighboring island 3 decays more rapidly and decays again after island 3 has disappeared.

Fig. 4 shows an Arrhenius plot of the decay rate of islands at their later stage in life. All data refer to islands of the same size of 1600 atoms. This particular size has been chosen because for smaller islands too few data points were available for a

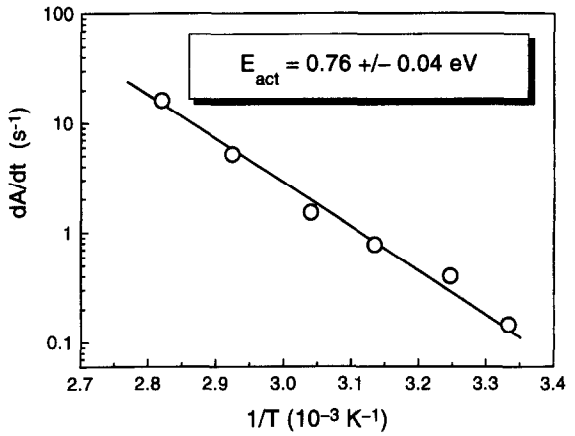

Fig. 4. Arrhenius plot of the average decay rate at a fixed size of 1600 atoms. Each data point represents the average decay rate of about 20 islands extracted from about 200 STM images. The slope corresponds to an energy of $E_{act}=0.76\pm0.04$ eV.

reasonable fit while for larger islands the effect of neighboring islands is too important. The data in Fig. 4 fit to an activation energy of 0.76 ± 0.04 eV. Save for a small correction from the line tension, this energy is the sum of the energy for the formation of an adatom on the terrace from a step and the activation energy for diffusion on the terrace, as we shall see shortly.

4. Theoretical analysis

4.1. General considerations

This section briefly recalls the elements of the continuum theory of Ostwald ripening in two dimensions [15,16]. Adatom islands represent a nonequilibrium state of the surface. The islands are produced in a nucleation process during deposition when the adatom density on the terrace is higher than a critical density ρ_{crit} above which nucleation takes place (see [4] for a review). This paper focuses on the decay after the deposition was terminated. It is assumed in the following that adatoms and not vacancies are the carriers of the mass transport between islands. This is a reasonable assumption since on an (111) surface the diffusion of adatoms is much faster than the diffusion of vacancies [17,18]. We note that vacancies appear to be the dominant mass transporting species in the island decay on Cu(100) [19].

The driving force for the time evolution of the size of islands is the difference in the chemical potential μ_{is} of the islands, i.e. the partial derivative of the free energy F of an island with respect to the number of particles N_{is} in the island. The free energy of an island changes with the number of particles in the island because the length of the perimeter changes. At the temperatures of interest here, the perimeter consists of (100) and (111) steps. Since the islands have a nearly hexagonal shape (Figs. 1 and 2), the free energy per step length for the (100) and the (111) type steps must be identical within a few percent. The chemical potential for these hexagonal islands is then

$$\mu_{is}=\frac{\partial F}{\partial N_{is}}=\frac{2\tilde{\gamma}\Omega}{\sqrt{3}s}, \tag{2}$$

where s and $\tilde{\gamma}$ are the length of the side of a hexagon and the line tension, respectively, and Ω is the area per atom. Eq. (2) is strictly valid only at $T=0$ and the line tension is then equal to the step energy per length. At higher temperatures, the chemical potential can be expressed in terms of the local line tension $\tilde{\gamma}(r)$ at any point on the perimeter and the radius of curvature r_k there:

$$\mu_{is}=\tilde{\gamma}(r)\frac{\Omega}{r_k}. \tag{3}$$

In the following, we analyze the island decay as if the islands had a circular shape. The equivalent radius R_i of a circular island with the same area as a hexagonal island of a side length s is

$$R_i=s\sqrt{\frac{3\sqrt{3}}{2\pi}}. \tag{4}$$

The chemical potential of such an equivalent island is

$$\mu_{is}=\alpha\frac{\tilde{\gamma}\Omega}{R_i}\quad\text{with}\quad\alpha=\sqrt{\frac{2\sqrt{3}}{\pi}}, \tag{5}$$

in which α is a shape parameter of the order of one. The chemical potential for quadratic islands

at $T=0$ is likewise easily derived. The result is

$$\mu_{is}=\frac{2\tilde{\gamma}\Omega}{s}, \tag{6}$$

with s the length of the side of the square. For islands on a quadratic lattice, a simple analytical solution of the island shape at any temperature is available in the Ising model [20]. By calculating the curvature of the quasi straight sections of the perimeter and after inserting the line tension of a straight step [21] it is straightforward to show that Eq. (6) is correct in the limit $\gamma_0 \ll k_B T$. The finite temperature corrections are of the order of $\exp(-\tilde{\gamma}a/k_B T)$ with a the diameter of an atom. For copper, these corrections are small at room temperature. From this result we infer that Eq. (5) is also a good approximation for the chemical potential of hexagonal islands at room temperature.

Using Eq. (2) and the standard expression for the chemical potential of lattice gas particles in the limit of small concentrations ρ_{ad}:

$$\mu=E_{ad}+k_B T \ln \rho_{ad}, \tag{7}$$

the equilibrium concentration of adatoms near the edge of hexagonal islands becomes

$$\rho_{ad}=e^{-\frac{E_{ad}-\alpha\tilde{\gamma}\Omega/R_i}{k_B T}}, \tag{8}$$

in which k_B is the Boltzmann constant and E_{ad} is the energy to create an adatom from a step (precisely from a kink in a step). We note that there is a principal difference in the chemical potential of a straight step and a curved step such as the perimeter of an island. The difference is because the emission of adatoms from a kink in a straight step does not change the macroscopic length of the step while removing atoms from a curved step does change the length of the step.

A theoretical description of island decay is most straightforward when one is in either one of the two limiting cases, the attachment–detachment limited case or the diffusion limited case (see, for example, [15]). In the attachment–detachment limited case, the detachment of the atoms from the step edge is much slower than the diffusion away from the island and vice versa. This case is realized if one has an extra activation barrier E_{det} which the detaching atoms must overcome in order to arrive on the terrace (Fig. 5). Theoretical calculations [22] as well as experiments [23] show that such a barrier does not exist on metal surfaces (provided that adatoms and not vacancies are the mass transport carrying species) while on semiconductors such a barrier has been observed [24]. In the diffusion limit, the rate of the island decay is determined by the diffusion away from the island. The diffusion current density per length of the perimeter of the island is proportional to the concentration gradient:

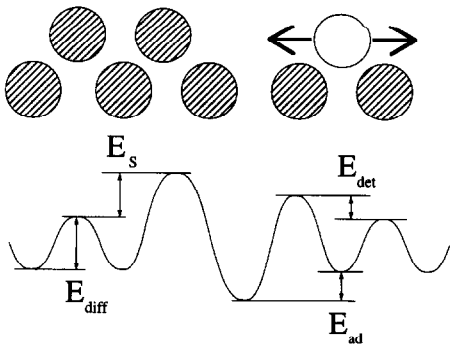

Fig. 5. Simplified potential energy curve for an adatom in the vicinity of an island edge. E_{diff} is the diffusion barrier on the terrace. The energy of formation of a terrace adatom is denoted by E_{ad}. If an additional barrier for the detachment from a step onto the terrace is present it is denoted by E_{det}. E_s is the Schwoebel–Ehrlich barrier which, if present, lowers the probability of an adatom crossing a step.

$$j=D\frac{\partial\rho_{ad}}{\partial r}, \tag{9}$$

with D the diffusion constant. The diffusion constant D can be expressed in terms of a hopping rate v for single jumps on a hexagonal lattice by

$$D=\frac{3}{2}a^2 v=\sqrt{3}\Omega v, \tag{10}$$

where a is the atom diameter. The rate by which the area of an island changes is then

$$\frac{\partial A}{\partial t}=-2\pi R_i\Omega_j=2\pi R_i\Omega D\frac{\partial\rho_{ad}}{\partial r}. \tag{11}$$

As long as the change in the island size is small on the time scale of the terrace diffusion, the concentration gradient at the island edge can be

calculated from the stationary solution of the diffusion equation, which is the Laplace equation. For the special geometry of an island inside a vacancy island and with some additional, though not necessarily realistic, simplifications, one can derive an analytical solution for the island decay which is Eq. (1) with an exponent $\kappa = 2/3$ [1,8,15]. In general, the description of island decay in the diffusion limit requires a numerical calculation of the (mean) concentration gradient perpendicular to the island edge at each time step during the life of an island. In summary, in the diffusion limit the island decay is determined by the following energies: the formation energy of adatoms from kinks in a straight step, the line tension and the activation energy for diffusion on the terraces. For islands in the vicinity of a descending step, the Schwoebel–Ehrlich barrier also has an influence on the decay. The appealing feature of quantitative studies on the island decay is that three of these energies can be determined from the experiment, as we shall see.

4.2. Method of the numerical analysis

We have determined the gradient of the adatom concentration on the terrace under the assumptions that: (1) the mass transport around the perimeter of the islands is much faster than the transport away from the island; (2) the flux away from the islands is slow on the time scale necessary for the adatom concentration to assume a stationary state; and (3) the islands remain at their position during the decay.

Experiments indicate that the first assumption is well fulfilled. By virtue of the motion of islands, every once in a while a coalescence of islands was observed. Whenever such an event occurred, the islands assumed their equilibrium shape on a time scale much faster than the time scale of island decay. The second assumption, the stationarity of the concentration profile, requires a brief consideration of the time scales on which the island size changes in relation to the time required for a change in the concentration profile. Because of the island decay, the position of the perimeter of an island moves in time. In order to have quasi-stationary conditions for the concentration profile, the motion of the position of the perimeter because of the shrinking island size must be slow compared to the motion of a diffusion front. This condition is most conveniently expressed as

$$\frac{\mathrm{d}R_i^2(t)}{\mathrm{d}t} \ll \frac{\mathrm{d}\Delta x_{\mathrm{diff}}^2}{\mathrm{d}t} = Dt, \tag{12}$$

in which R_i is the radius of the island as before, $\Delta x_{\mathrm{diff}}^2$ describes the motion of a diffusion front and D is the diffusion coefficient. With the help of standard analytical solution for the island decay in the specific geometry of an island in a vacancy island [1,15], one obtains the condition

$$\frac{\mathrm{e}^{-E_{\mathrm{ad}}/k_{\mathrm{B}}T}}{\ln(R_i/R_a)} \frac{\alpha\tilde{\gamma}\Omega}{R_i k_{\mathrm{B}} T} \ll 1. \tag{13}$$

Here, E_{ad} denotes the energy for the formation of an adatom as before, $\tilde{\gamma}$ is the line tension and α is the same as defined in Eq. (5), and R_i and R_a, are the radii of the island and the vacancy island, respectively. It is easily seen that Eq. (13) is well fulfilled for all radii R_i relevant in our case. Hence, it is legitimate to calculate the flux away from the islands from the solution of the stationary concentration profile using the chemical potential at the perimeters of the islands as boundary conditions [Eq. (5)].

The assumption that the islands remain at their initial positions while decaying is not fulfilled. On the contrary, even at room temperature the islands wander about considerably during their lifetime. The incorporation of this wandering process into the simulations would present a formidable effort. In our simulations, we have assumed that the islands stay at their initial positions. As a consequence, no perfect match between the experimental and simulated decay curves can be expected, even for a correct set of parameters. Since the wandering of islands is stochastic, it is legitimate to search for the optimum set of parameters by minimizing the mean square deviations of quantities characterizing the decay.

The question whether the true, nearly hexagonal, equilibrium shape must be used in the simulations instead of circular islands requires an additional consideration. Clearly, one expects a larger concentration gradient near the edges of a hexagonal

island compared with the gradient at the straight sections. We have found that the difference in the gradient is in fact larger than a factor of two. In order to analyze whether this has an effect on the decay time and the shape of the decay curves, we have performed model studies for hexagonal and round islands. It was found that hexagonal and round islands of the same area decay in the same time and with the same shape of the decay curve when they are placed in a larger vacancy island. Differences are expected to become larger when the distances between islands or between islands and steps become small compared with the radii of the islands. For simplicity, we have nevertheless performed the simulations using circular islands.

All simulations were performed on a 256×256 grid. The stationary concentration was calculated for each time step by solving the Laplace equation using the standard over-relaxation algorithm [25]. The algorithm was found to have converged sufficiently when the relative change in the concentration gradient from one cycle to the next was less than 10^{-5}. The concentration gradient normal to the perimeter was averaged along the perimeter of each island and the flux calculated accordingly. This flux determines the island sizes in the next step of iteration. We note that the procedure described above is not mass conserving. Firstly, the small change in the position of steps due to the island decay is not explicitly considered. More importantly, the method can lead to unrealistic increases in the sizes of larger islands if a small island is in the vicinity and if the calculated flux from the small island is such that the island would disappear in the early stages of the following time step. We have curtailed such unrealistic growth using a simple constraint.

As discussed before, there is a strong indication that steps on the (111) surface bear a Schwoebel–Ehrlich barrier which hinders the hopping of atoms over a step edge. If this barrier completely blocks the motion of atoms over a descending step, the step does not set a boundary condition for the concentration on the upper terrace. If the Schwoebel–Ehrlich barrier is finite, the boundary condition is the continuity of the current across the step. The algorithm in that case is easily derived. Suppose one has a step along the y-axis between the positions x_n and x_{n+1}, where x_n and x_{n+1} denote the last and first position on the upper and lower terrace, respectively. The diffusion current towards the step edge from the upper side is

$$j \propto \nu[\rho(x_{n-1}) - \rho(x_n)]. \tag{14}$$

The diffusion current over the step edge is

$$j \propto \nu_s[\rho(x_n) - \rho(x_{n+1})], \tag{15}$$

with ν_s the hopping rate over the Schwoebel–Ehrlich barrier. The concentration at the lower edge of the step is equal to the equilibrium concentration at the (straight) edge ρ_{eq} [Eq. (8) with $R_i = \infty$]. Hence, the Schwoebel–Ehrlich barrier is taken into account by replacing the standard algorithm for the solution of the Laplace equation [25] (in Cartesian coordinates):

$$\rho(x_n, y_n) = \frac{1}{4}[\rho(x_{n-1}, y_n) + \rho(x_{n+1}, y_n) + \rho(x_n, y_{n-1}) + \rho(x_n, y_{n+1})] \tag{16}$$

by

$$\rho(x_n, y_n) = \frac{\rho(x_n, y_{n-1}) + \rho(x_n, y_{n+1})}{3 + \nu_s/\nu} + \frac{\rho(x_{n-1}, y_n) + \rho_{eq}\nu_s/\nu}{3 + \nu_s/\nu}. \tag{17}$$

We assume that the pre-exponential factor for the hopping over the Schwoebel–Ehrlich barrier is the same as the one for the hopping over the terrace so that

$$\frac{\nu_s}{\nu} = e^{-E_s/k_B T}, \tag{18}$$

where E_s is the barrier height (Fig. 5).

The boundary conditions at the edges of the simulation frame constitute a more severe technical problem. The chemical potential at the boundary depends on the island sizes surrounding the frame. The chemical potential changes, therefore, as time progresses. The sizes of the islands surrounding the frame are not known, however. Neither experimentally because one typically observes the decay within a fixed frame, nor in the simulations because no islands are defined outside the frame. Initially,

we have performed simulations for a subsection of an island distribution on a large terrace. We have assumed that the chemical potential at the edge of the simulation frame was equal to the mean chemical potential within the frame. We found that this boundary condition fails to provide a correct description of the decay for all but the early decaying innermost islands for which the chemical potential was entirely determined by the surrounding islands. We have therefore simulated the island decay for an arrangement of islands on relatively small terraces where the steps set defined boundary conditions (Fig. 2). A vanishing gradient of the concentration parallel to the steps was assumed for the edges of the frame perpendicular to the step direction.

4.3. Results of the simulation

The key parameter which determines the shape of the island decay curves as well as the relative lifetimes times of the islands is the line tension $\tilde{\gamma}$. Following the simplest analytically solvable model for the island decay, we characterize the shape of the decay curve by a parameter κ [Eq. (1)] which is obtained by matching the entire decay curves to a power law.

Since the island decay does not obey this simple power law, κ has merely the meaning of a parameter which characterizes the shape of the decay curves. It serves for a comparison of the experimental curves to the simulation, provided that the match to Eq. (1) is performed in the same manner. As remarked before (Table 1), the exponents κ vary substantially from island to island, highlighting the fact that the shape of the decay curve depends significantly on the environment of an island. The comparison of the shape parameters κ between experiment and simulation opens up the possibility to determine a best fit value for the line tension $\tilde{\gamma}$. In Fig. 6, the mean square deviation of the shape parameters:

$$\langle(\Delta\kappa)^2\rangle=\langle(\kappa_{\mathrm{exp}}-\kappa_{\mathrm{sim}})^2\rangle \tag{19}$$

is plotted versus the line tensions for three different values E_s for the Schwoebel–Ehrlich barriers. The optimum values for the line tension $\tilde{\gamma}$ is obtained by fitting parabolas to the data. The optimum

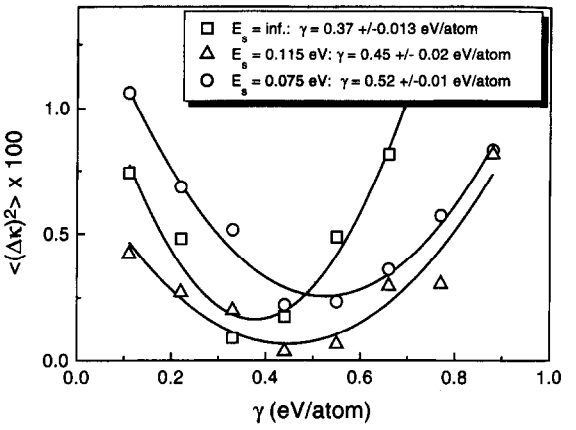

Fig. 6. Mean square deviation of the shape parameter κ as a function of the line tension $\tilde{\gamma}$. The parameter is the value E_s for the Schwoebel–Ehrlich barrier.

values depend on the assumed barrier with the trend to larger values of $\tilde{\gamma}$ for smaller E_s. This is a reasonable result since a lower value for E_s makes an upper step edge a more effective sink for adatoms and an island placed near a straight step has a larger decay exponent (Table 1). To compensate for that, a larger value for the line tension must be assumed which reduces the shape parameter κ.

Simulations with no Schwoebel–Ehrlich barrier fail to describe the correct relative lifetimes of the islands. In particular islands near a descending step such as island 3 in Fig. 2 disappear earlier in reality. We have therefore varied the Schwoebel–Ehrlich barrier E_s in the simulations and searched for an optimum in the mean square deviation of the relative lifetimes:

$$\langle(\Delta t)^2\rangle=\left\langle\left(\frac{\tau_{\mathrm{exp}}}{\tau_{\mathrm{exp}}(8)}-\frac{\tau_{\mathrm{sim}}}{\tau_{\mathrm{sim}}(8)}\right)^2\right\rangle, \tag{20}$$

assuming a line tension $\tilde{\gamma}=0.45$ eV/atom (Fig. 7). The lifetime of island 8, $\tau_{\mathrm{exp}}(8)$, serves as a reference in experiment and simulation. The mean square deviation has a minimum at

$$E_s=0.116\pm0.002\ \mathrm{eV}. \tag{21}$$

From Fig. 6 we see that the optimum line tension for this value of E_s is

$$\tilde{\gamma}=0.45\pm0.02\ \mathrm{eV/atom}. \tag{22}$$

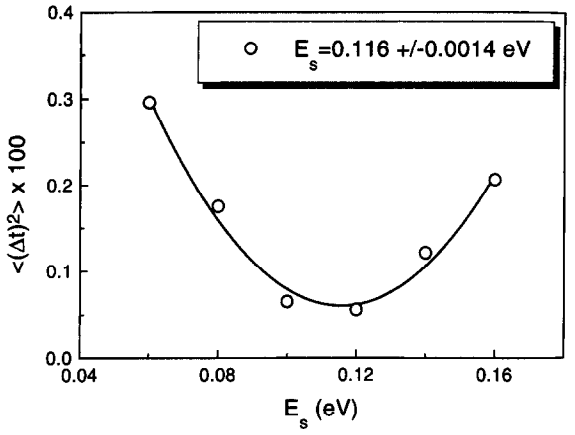

Fig. 7. Mean square deviation for the relative life times of the islands as a function of the value E_s of the Schwoebel–Ehrlich barrier. The minimum is at 0.116 eV.

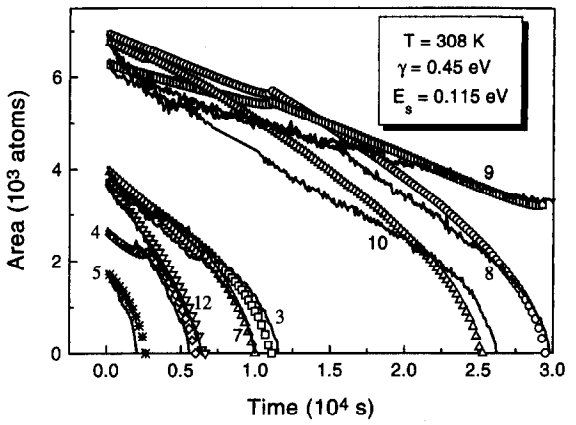

Fig. 8. Comparison of the best fit simulation (symbols) and experimental (solid lines) data. The numbers refer to the islands in Fig. 2.

The errors for E_s and $\tilde{\gamma}$ in Eqs. (21) and (22) are the statistical errors in fitting a parabola to the mean square deviation. The true error is certainly larger but more difficult to assess. In order to have a better feeling for the magnitude of the systematic error we have analyzed a second set of 8 islands on a single, larger terrace at a temperature of 319 K. For this set we found $E_s = 0.14$ eV and $\tilde{\gamma} = 0.5$ eV/atom. The slightly higher value for E_s obtained from this second set may not be significant because of the single descending step involved. In consideration of the difference in E_s and $\tilde{\gamma}$ between the two simulations and because of the relatively broad minimum in the fits (see Figs. 6 and 7) we believe that a true error may be as large as ± 0.02 and ± 0.1 eV for E_s and $\tilde{\gamma}$, respectively. Our analysis did not account for the random walk of the islands while they decay. We assume that the error introduced by the random walk is of a statistical nature and has no systematic effect on the value of the line tension and the Schwoebel–Ehrlich barrier obtained from the analysis. The imperfection of the fit between the simulated decay curves and the experiment in Fig. 8, however, is attributed to the random motion of the islands.

The overall agreement between experiment and simulation is demonstrated in Fig. 8. The time of the simulation is scaled to the experimental time by matching the death time for island 8. The agreement is quite satisfactory. We have included the decay of island 9 in Fig. 8, although this island was not included in the optimization process since it is still present at the termination of the experiment. The decay of island 9 is entirely due to the finite Schwoebel–Ehrlich barrier. According to the simulations, the island would not decay at all if the Schwoebel–Ehrlich barrier were infinitely large. On the other hand, the island would die before island 8 if there was no Schwoebel–Ehrlich barrier at all. The decay of island 9 is therefore a sensitive measure of the Schwoebel–Ehrlich barrier. The good agreement between experiment and the simulation is therefore an independent confirmation that we have determined the Schwoebel–Ehrlich barrier.

The factor by which the simulation time has to be expanded to match the experimental time fixes the ratio of the diffusion currents in the simulation and the experiment. From the simulation in Fig. 8 and the activation energy for the island decay rate at constant island size (Fig. 4) the pre-exponential factor for the adatom diffusion is determined as

$$\nu_0 = 25 \times 10^{11 \pm 0.65}\ \mathrm{s}^{-1}. \tag{23}$$

The error reflects the error in the determination of the activation energy in Fig. 4. In addition to the experimental error, there is a 50% systematic error since the simulations where performed on a square lattice rather than on a hexagonal lattice.

5. Discussion

The result which is most straight forward to discuss is the sum of the energy for the formation of an adatom on the terrace and the activation energy for the diffusion. In Fig. 4, we have found an activation energy of $E_{act}=0.76\pm0.04$ eV. Save for a small correction which arises from the line tension [Eq. (8)], this energy is equal to the sum of the energy of formation of adatoms from kinks in a straight step E_{ad} and the activation barrier for diffusion on the terraces E_{diff}. In Fig. 4, we have plotted the derivative of the area with respect to time for islands having 1600 atoms. After inserting the equivalent radius of such islands in Eq. (8) and by using the line tension one obtains

$$E_{ad}+E_{diff}=E_{act}+\alpha\tilde{\gamma}\Omega/\sqrt{1600\Omega/\pi}$$
$$=0.78\pm0.04\ \text{eV}. \quad (24)$$

According to EMT (effective medium theory) calculations in the lowest level of approximation [16] the activation energy for diffusion is $E_{diff}=0.053$ eV and the energy for the formation of an adatom from a kink is $E_{ad}=0.714$ eV. The sum 0.77 eV is in excellent agreement with our results.

The value for the Schwoebel–Ehrlich barrier, $E_s=0.12$ eV, is similar to the barrier found by Morgenstern et al. [8] on Ag(111) surface (0.13 eV). In Ref. [8], the barrier was determined from the rate by which vacancy islands are filled. These vacancy islands have (100) and (111) oriented steps of equal length with a large kink concentration near the corners of the islands. According to a theoretical study [26] the Schwoebel–Ehrlich barrier on Ag(111) should be significantly lower for (111) type steps than for the (100) steps. The calculated values for straight steps are $E_{s(111)}=0.06$ eV and $E_{s(100)}=0.28$ eV. For both step orientations the numbers are smaller for kink sites. The value obtained by Morgenstern et al. is a (weighted) average over steps of different orientations and is insofar not directly comparable with our result which is obtained for the straight steps in Fig. 2 which are of the (100) type.

As we have already pointed out, the late stage of the decay does show a scaling behavior of $A(t)\propto t^{\alpha}$. While it would have been possible to fit this exponent directly to the simple analytical solution for the diffusion limited decay as in Ref. [1], this procedure did not appear reasonable in view of the large variation in the exponent from island to island. An evaluation of the line tension from the decay exponent is meaningful only if the environment of the islands is taken into account, or if islands in a well defined geometry are studied [8].

The value of the line tension of $\tilde{\gamma}=0.45$ eV/atom should approximately represent the step energy. Surprisingly, the value is more than a factor of two larger than expected. According to EMT calculations in the lowest level of approximation, the step energy is 0.208 eV for steps on a Cu(111) surface [17]. This value is in rough accordance with a compilation of step energies from various experimental and theoretical sources [27]. A similar but smaller discrepancy was found by Morgenstern et al. for Ag(111) [1,8]. We consider it as rather unlikely that the discrepancy can be attributed to inaccuracies of the fitting procedures or to the assumptions made in the simulations. A possible source of error to be considered could be a break down of the continuum approximation. The line tension $\tilde{\gamma}$ is determined from the effective exponent κ which characterizes the shape of the decay curves. The value of κ depends to a large extend on the shape of the decay curve in the late stage of the life of an island where the island size is already small. It is not inconceivable that fitting the experimental κ to a continuum theory could cause a systematic error in line tension.

In summary, we have shown that the island decay on Cu(111) can be understood in terms of the diffusion limited decay mechanism. From the temperature dependence the sum of the energy for the formation of an adatom from a kink and the activation energy for diffusion on the terraces was found and the result is in excellent agreement with theoretical calculations. Detailed simulations of the island decay at constant temperature yielded a value for the Schwoebel–Ehrlich barrier and the line tension.

Acknowledgements

The authors acknowledge fruitful discussions with N.C. Bartelt, Ch. Klünker and G. Rosenfeld.

The computer code for the determination of the island sizes in the STM images was developed by J.B. Hannon. The work was partially supported by the Fond der Chemischen Industrie.

References

[1] K. Morgenstern, G. Rosenfeld, G. Comsa, Phys. Rev. Lett. 76 (1996) 2113.
[2] T.A. Pal'chevskaya, V.M. Belousov, L.V. Bogutskaya, Theor. Exp. Chem. 31 (1995) 203.
[3] E.A. Dobisz, F.K. Perkins, S.L. Brandow, J.M. Calvert, C.R.K. Marrian (Eds.), in: Conference on Materials-Fabrication and Patterning at the Nonoscale, 1995.
[4] M. Zinke-Allmang, L.C. Feldman, M.H. Grabow, Surf. Sci. Rep. 16 (1992) 377.
[5] G. Meyer, J. Wollschläger, M. Henzler, Surf. Sci. 231 (1990) 64.
[6] G. Meyer, B. Voigtländer, Surf. Sci. Lett. 274 (1992) L541.
[7] M.D. Johnson, C. Orme, A.W. Hunt, D. Graff, J. Sudijono, L.M. Sander, B.G. Orr, Phys. Rev. Lett. 72 (1) (1994) 116.
[8] K. Morgenstern, G. Rosenfeld, E. Lægsgaard, F. Besenbacher, G. Comsa (to be published).
[9] G. Ehrlich, F.G. Hudda, J. Chem. Phys. 44 (1966) 1039.
[10] R.L. Schwoebel, E.J. Shipsey, J. Appl. Phys. 37 (1966) 3682.
[11] A.F. Becker, G. Rosenfeld, B. Poelsema, G. Comsa, Phys. Rev. Lett. 70 (1993) 477.
[12] H.A. van der Vegt, H.M. van Pinxteren, M. Lohmeier, E. Vlieg, Phys. Rev. Lett. 68 (1992) 3335.
[13] K.H. Besocke, Surf. Sci. 181 (1987) 145.
[14] G. Schulze Icking-Konert, M. Giesen, H. Ibach (to be published).
[15] P. Wynblatt, N.A. Gjostein, in: J.O. McCaldin, G. Somorjai (Eds.), Progress in Solid State Chemistry, vol. 9, Pergamon Press, Oxford, 1975, p. 21.
[16] B.K. Chakraverty, J. Phys. Chem. Sol. 28 (1967) 2401.
[17] P. Stolze, J. Phys. Cond. 6 (45) (1994) 9495.
[18] M. Karimi, T. Tomkowski, G. Vidali, O. Biham, Phys. Rev. B 52 (1995) 5364.
[19] J.B. Hannon, C. Klünker, M. Giesen, H. Ibach, N.C. Bartelt, J.C. Hamilton, Phys. Rev. Lett. 79 (1997) 2506.
[20] M. Breeman, G.T. Barkema, D.O. Boerma, Surf. Sci. 323 (1995) 71.
[21] N.C. Bartelt, T.L. Einstein, E.D. Williams, Surf. Sci. 312 (1994) 411.
[22] R. Stumpf, M. Scheffler, Phys. Rev. Lett. 72 (1994) 254.
[23] G. Ehrlich, Surf. Sci. 331–333 (1995) 865.
[24] W. Theis, N.C. Bartelt, R.M. Tromp, Phys. Rev. Lett. 75 (1995) 3328.
[25] H. Ibach, Electron Energy Loss Spectroscopy, Springer Series in Optical Sciences 63, Springer, Berlin 1991.
[26] Yinggang Li, A.E. DePristo, Surf. Sci. 319 (1994) 141.
[27] H.P. Bonzel, Surf. Sci. 328 (1995) L571.